Available online at www.sciencedirect.com
SCIENCE DIRECT®
Biochimica et Biophysica Acta 1661 (2004) 178–187
BIOCHIMICA ET BIOPHYSICA ACTA
BBA
www.bba-direct.com

# Farnesol-DMPC phase behaviour: a $^2$H-NMR study

Amy C. Rowat[a], James H. Davis[b,*]

[a] *MEMPHYS, Center for Biomembrane Physics, Department of Physics, University of Southern Denmark, Campusvej 55, DK-52 30 Odense, Denmark*
[b] *Department of Physics, University of Guelph, 211 MacNaughton, Guelph, ON, Canada N1G 2W1*

Received 3 September 2003; received in revised form 16 December 2003; accepted 9 January 2004

**Abstract**

Involved in a number of diverse metabolic and functional contexts, farnesol is a central component of the mevalonate pathway, post-translationally attaches to proteins, and affects a number of other membrane-associated events. Despite farnesol's biological implications, a detailed analysis of how farnesol affects the physical properties and phase behaviour of lipid membranes is lacking. As $^2$H-NMR spectra are sensitive to molecular motions and acyl chain orientation, they can be used to measure the degree of molecular order present in the system. Also, since the $^2$H-NMR spectra of fluid and gel phase lipids are very different, they are sensitive probes of membrane phase equilibrium and can be used to determine fluid–gel phase boundaries. In this study, dimyristoyl phosphatidylcholine-$d_{54}$ (DMPC-$d_{54}$) bilayers containing varying concentrations of *trans–trans* farnesol (2.5–20.0 mol%) are investigated over a range of temperatures (8–30 °C). Analysis of these spectra has led to the construction of a farnesol-DMPC-$d_{54}$ temperature–composition plot. We show that increasing concentrations of farnesol induce a decrease in the fluid–gel phase transition temperature and promote fluid–gel coexistence. Interestingly, farnesol does not seem to affect the quadrupolar splittings ($\Delta\nu_Q$) in the fluid phase, i.e., the organization of farnesol within the bilayer and its interaction with phospholipids does not appreciably influence acyl chain order in the fluid phase.


*Keywords:* Membrane; Lipid bilayer; Isoprenoid; $^2$H-NMR; Phase equilibria

## 1. Introduction

From its non-specific action upon the activity of various ion channels [1–4] to its effect in preferentially inducing apoptosis in cancer cells [5–7], farnesol is implicated in a large variety of membrane-related biological processes. This 15-carbon isoprenoid (Fig. 1) plays a vital role in the mevalonate pathway—it is the precursor of sterols, dolichol, and vitamins E and $K_1$ and may regulate cholesterol synthesis through its interaction with 3-hydroxy-3-methyl-glutaryl-coenzyme A (HMG-CoA) reductase [8–10]. Farnesol also plays a role in the regulation of gene expression [11,12].

Furthermore, a wide range of proteins (including Ras, nuclear lamins, and the γ-G-protein subunit) are post-translationally modified by farnesol. Farnesylation renders proteins functionally active and targets their association with the membrane, a necessary step in both protein function and signal transduction [13–15]. The biological activity of farnesol is well recognized, yet to date, there have been very few biophysical studies of how this compound interacts with membranes.

Investigations of the conformation and dynamics of isoprenoid probes (including farnesol) in membranes by electron paramagnetic resonance (EPR) [16,17] and deuterium nuclear magnetic resonance ($^2$H-NMR) [18,19] attest to farnesol's integration into the lipid bilayer but haven't provided much insight into how farnesol affects membranes. Using calorimetry, it has been demonstrated that farnesol influences the physical properties of DMPC bilayers. In particular, the main fluid–gel phase transition temperature ($T_m$) is lowered and broadened [20]. In general, how the introduction of branched compounds affects membrane phase behaviour and lipid acyl chain order in the membrane's fluid phase remains unclear. Increasing concentrations of farnesol have been reported to decrease fluorescence anisotropy in extracted human leukemia CeM-C1 cell membranes [20], yet a $^2$H-NMR study has indicated that incorporation of branched phytol or phytanic

* Corresponding author. Tel.: +1-519-824-4120x85; fax: +1-519-836-9967.
*E-mail address:* jhd@physics.uoguelph.ca (J.H. Davis).

0005-2736/$ - see front matter © 2004 Elsevier B.V. All rights reserved.
doi:10.1016/j.bbamem.2004.01.002

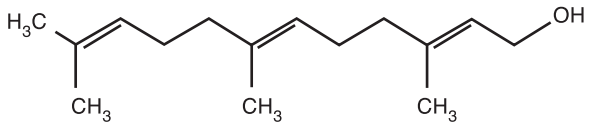


Fig. 1. Structure of *trans–trans* farnesol.

acid increases the order parameters of 1-palmitoyl(-stearoyl)-2-[$^2H_{31}$] palmitoyl-*sn*-glycero-3-phosphocholine (PC-$d_{31}$) membranes [21]. These studies provide evidence that branched chain compounds like farnesol affect the membrane's physical properties, but there is a need for a more refined understanding of how farnesol influences lipid phase behaviour on a molecular level.

Deuterium NMR ($^2$H-NMR) provides an excellent method of learning more about lipid acyl chain conformation, orientational order and dynamics. Bilayer membranes exhibit a broad spectrum of molecular motions such as lateral and axial diffusion, chain isomerization, and local bilayer director fluctuations. Motions which are fast on the spectroscopic time scale will average or reduce the quadrupolar interaction. In the limit of rapid isotropic reorientation, for example, the quadrupolar splittings ($\Delta\nu_Q$) are reduced to zero. In contrast, at sufficiently low temperatures the quadrupolar splittings reach their maximum value $\Delta\nu_Q = 126$ kHz. In this way the degree of motional averaging is reflected in the shape and breadth of the NMR spectrum. For chain perdeuterated lipids, a narrow spectrum consisting of a superposition of powder pattern line shapes with well-defined doublets ($\Delta\nu_Q$ from 1 to 30 kHz) is characteristic of the fluid phase. In the gel phase the individual doublets are not resolved, resulting in a characteristically broad, bell-shaped spectrum having splittings of about 63 kHz and smoothly rounded shoulders. Provided that molecules do not exchange between domains on the spectroscopic time scale, the coexistence of gel and fluid phases is seen as the super position of these characteristic gel and fluid phase spectra. NMR is thus a useful tool for monitoring the phase behaviour and phase boundaries of lipid mixtures [22–26]. Information obtained from such studies provides a basis for the understanding not only of the lateral organization of membranes but also of the molecular interactions between membrane components. Until now no thorough analysis of farnesol-DMPC phase behaviour has been undertaken.

In this paper, we present a $^2$H-NMR study of *trans–trans* farnesol in dimyristoyl phosphatidylcholine-$d_{54}$ (DMPC-$d_{54}$) bilayers in the presence of excess phosphate buffer. Farnesol is found to decrease the main phase transition temperature ($T_m$) and induce a broad gel-phase coexistence region. In the fluid phase, farnesol does not significantly alter the acyl chain quadrupolar splittings even up to concentrations of 20 mol%. The temperature–composition plot obtained illustrates farnesol's marked effects upon the phase behaviour of DMPC bilayers.

## 2. Methods

### 2.1. Sample preparation

*Trans–trans* farnesol (96%) and organic solvents were products of Sigma-Aldrich (Oakville, ON). DMPC-$d_{54}$ was obtained from Avanti Lipids (Birmingham, AL) and used without further purification. Farnesol was dissolved in ethanol to create a stock solution (1.46 mg/ml). DMPC-$d_{54}$ was then dissolved in appropriate volumes of this solution to produce samples of varying farnesol concentrations [2.5–20 mol%]. Samples were rotovapped for about 30 min and there-after placed in a vacuum for at least 12 h to evaporate all traces of solvent. Accurately weighing the sample before and after solvent evaporation confirmed that farnesol does not evaporate during this process. The dried lipid–farnesol mixture was transferred to an Eppendorff tube. A potassium phosphate monobasic-sodium hydroxide buffer (0.05 M, pH $7.00 \pm 0.01$ at 25 °C, Fisher Scientific, Nepean, Canada) was added at a 4:3 lipid/buffer weight to volume ratio. Using a thin glass stirring rod, the sample was alternately mixed and centrifuged until homogeneous; it was then spun down into small glass tubes and tightly sealed with a red rubber stopper (Fisher Scientific). The total sample mass was consistently between 60 and 80 mg. In the case where the lipid mass was significantly less than this, the number of scans was increased to achieve a similar signal-to-noise ratio.

### 2.2. $^2$H-NMR methods

Spectra were acquire data frequency of 76.77 MHz on a 500 MHz Bruker Avance Spectrometer (Bruker Bio spin, Milton, ON). Experiments were run from higher to lower temperatures (typically from 30 to 8 °C). Samples were equilibrated for 15 min before the first scan and at least 10 min between temperatures. A quadrupolar echo pulse sequence [27] was used with a 90° pulse length of 2.4 μs, pulse separation $\tau = 15$ μs, and repetition time of 1.5 s.

Acquisition was begun well before the top of the echo [28]. The number of scans varied depending on the phase of the sample: 512 scans were run on liquid crystalline samples while the gel phase required 1024 scans. Complex free induction decay signals (FIDs) were first phase-adjusted in the time domain so that the imaginary part of the signal was zero at the echo peak. The FIDs were then shifted so they were symmetric about the point of the echo maximum and points before the echo maximum were discarded [28,29]. A Fourier transform then yields a frequency spectrum with an undistorted baseline [30]. With the baseline corrected to have zero average value, the *N*th moment was calculated using the expression

$$M_N = \frac{\int_{-\omega_L}^{+\omega_L} f(\omega)\,|\,\omega\,|^N d\omega}{\int_{-\omega_L}^{+\omega_L} f(\omega) d\omega} \quad (1)$$

where $f(\omega)$ is the experimental spectrum and $\pm\omega_L$ are the frequency limits of the spectrum. Oriented spectra were obtained from the powder spectrum by dePake-ing [31,32].

## 3. Results and discussion

Spectra characteristic of DMPC-$d_{54}$ in both the fluid and gel phase are illustrated in Fig. 2A and B. Above $T_m$, the quadrupolar splitting ($\Delta\nu_Q$) can range from $\sim$ 1 kHz for the terminal methyl group to $\sim$ 25 kHz for the methylene groups near the lipid–water interface. Peaks arising from the methyl and many of the methylene groups are well-resolved. The variation of these splittings with chain position is due to the gradient in molecular motion and chain flexibility characteristic of the lipid bilayer fluid phase. Immediately below $T_m$, the spectrum becomes much broader (methylene group splittings $\Delta\nu_Q$ $\sim$ 60 kHz) and less finely structured. As the lipid chains become more restrained in their motions, the dynamical time scales become comparable to the NMR time scale. Consequently, the line width of each individual quadrupolar doublet is larger and the methylene peaks are not as distinctly resolved. The transition from fluid to gel phase for pure DMPC-$d_{54}$ occurs over less than one degree in the range from 20.5 to 19.5 °C.

If the two types of domains occurring in a two-phase (fluid–gel) coexistence region are static, i.e., the molecules making up each of the two types of domain remain localized within that domain for times long compared to the NMR time scale, then the $^2$H-NMR spectra provide a simple quantitative means of measuring the properties of these domains. On the other hand, if one or both of the molecular components of these domains are free to exchange, by diffusion, between the two types of domains, then the situation is somewhat more complicated and the NMR spectra are more difficult to interpret. For example, in the present system, if farnesol rapidly diffuses in and out of both types of domains then the local concentration of farnesol within a particular domain may fluctuate with time. Within the two-phase region the thermodynamic character of either type of domain is quite sensitive to the concentration of farnesol. Consequently, the contribution to the $^2$H-NMR spectrum arising from lipids within such a domain will experience a broadening not present in domains of fixed composition. A similar effect arises if the DMPC molecules are free to exchange between types of domains on the NMR time scale. In that case the contribution to the NMR spectrum arising from those lipids will be averaged over the two environments. In the presence of exchange of either of the molecular components, the NMR spectrum will be somewhat broadened and it will become difficult to quantitatively separate the fluid and gel components of the NMR spectra within the two-phase coexistence region.

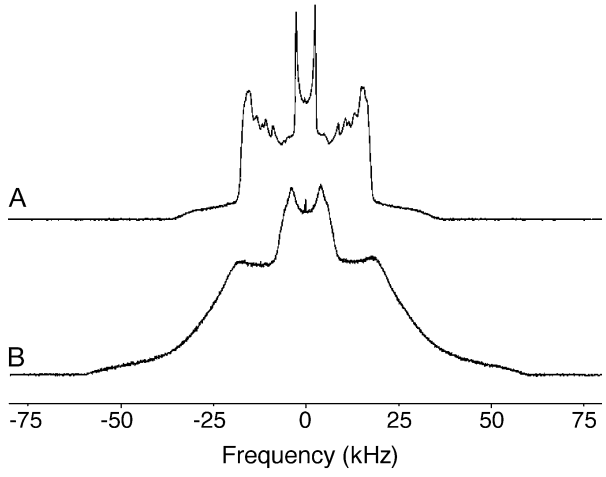


Fig. 2. $^2$H-NMR as a monitor of membrane phase behaviour: $^2$H-NMR spectra of DMPC-$d_{54}$ in excess buffer in (A) the fluid phase, $T$=20.5 °C, and (B) the gel phase, $T$=19.5 °C.

The addition of farnesol does, in fact, broaden the temperature range over which the phase transition occurs as it creates a fluid–gel coexistence region. Within this two-phase coexistence region, the NMR spectra do possess components characteristic of each of the gel and fluid phases. For example, the inclusion of 12.5 mol% farnesol (Fig. 3) results in a two-phase coexistence region covering a range of temperatures from $17.5 \pm 0.5$ to $9.5 \pm 1.5$ °C. As the temperature is lowered through this range, the ratio of gel to fluid components in the spectrum increases until the sharp peaks characteristic of fluidity disappear and the broad shoulders denoting the gel phase dominate the spectral line shape. Progressively increasing concentrations of farnesol broaden this two-phase region to a larger extent. Farnesol partitions preferentially into the fluid phase, stabilizes the fluid phase to lower temperatures, and promotes fluid–gel phase coexistence. This results in a depression of the onset of the main phase transition so that the two-phase line (fluidus) marking the boundary between the fluid phase and the two-phase coexistence region extends to lower temperatures as farnesol concentration is increased. This effect has also been observed using differential scanning calorimetry ([20], Rowat and Ipsen, private communication).

Farnesol's tendency to promote fluidity is illustrated in the concentration dependence shown in Fig. 4. At a given temperature within the two-phase coexistence region (e.g., at $T$=16 °C as in Fig. 4), the $^2$H-NMR spectra show that the proportion of fluid phase increases with farnesol concentration. At low concentrations (e.g., 2.5 mol%), the effects of farnesol appear subtle—the methyl peaks of this predominantly gel-phase spectrum grow slightly sharper and the broad gel phase shoulders become slightly more angular. At 5.0 mol% farnesol, these shoulders begin to peak. At a farnesol concentration of 7.5 mol%, it is evident that the spectrum contains two components, one characteristic of the gel phase, the other of the fluid phase. As farnesol content is further increased the intensity of the fluid phase component grows at the expense of the gel phase component. At and

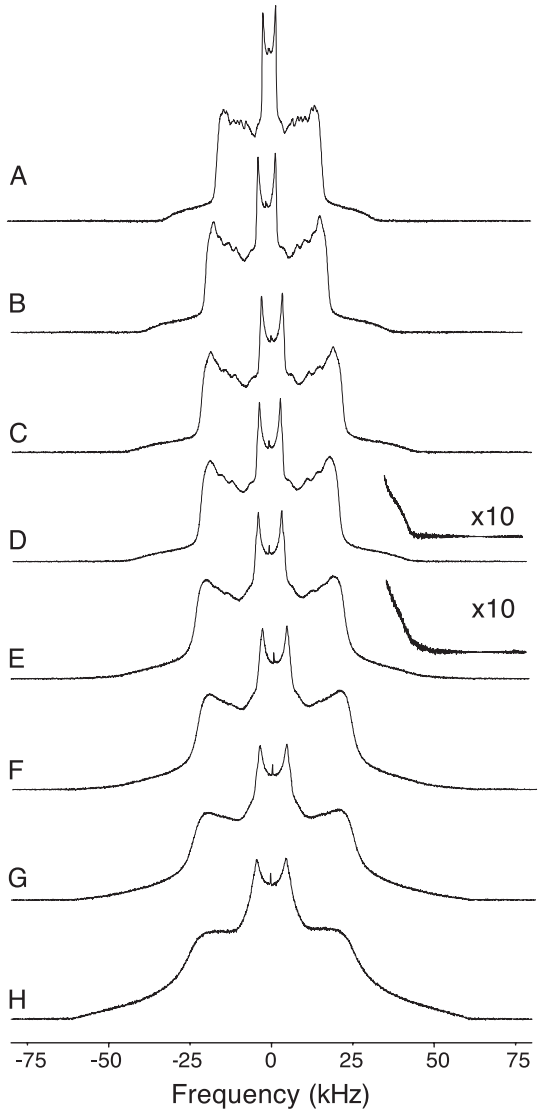


Fig. 3. $^2$H-NMR spectra illustrating the temperature dependence of 12.5 mol% farnesol in DMPC-$d_{54}$. (A) $T$=24.0 °C; (B) 19.0 °C; (C) 18.0 °C; (D) 17.0 °C; (E) 16.0 °C; (F) 15.0 °C; (G) 14.0 °C; (H) 11.0 °C.

above 15 mol% farnesol, the spectra at 16 °C are indicative of the fluid phase. While this behaviour is reminiscent of other model membrane systems, there is a significant difference between the $^2$H-NMR spectra observed here for the farnesol/DMPC fluid–gel coexistence region and those typically observed in the fluid–gel coexistence regions of DMPC/DSPC (1,2-distearoyl-*sn*-glycero-3-phosphocholine) [33], DPPC/cholesterol [34], or peptide/phospholipid [35,36]. In those studies, the two component spectra observed at any given temperature within the two-phase region could be readily decomposed using difference techniques [35] into endpoint spectra corresponding to the tie-line endpoint concentrations at that temperature within the two-phase coexistence region. In the case of farnesol/DMPC, inspection of the fluid phase component of the spectra obtained for different farnesol concentrations at a given temperature within the two-phase region (see Fig. 4) reveals that the fluid phase component of the spectra varies slightly with farnesol concentration. This is most easily seen by looking at the narrow doublet corresponding to the terminal methyl groups whose quadrupolar splitting decreases slightly with increasing farnesol concentration. In this situation, spectral subtractions are clearly impractical, since the component spectra are not independent of concentration, and the endpoint spectra and concentrations cannot be determined by difference spectroscopy. The fact that the fluid phase component of the spectra in this two-phase region is concentration-dependent is probably due to rapid exchange of molecules between the two coexisting types of domains. Since farnesol is significantly smaller than the phospholipid, it seems most likely that diffusion of farnesol between fluid and gel phase domains results in fluctuations in composition, blurring the distinction between the two types of

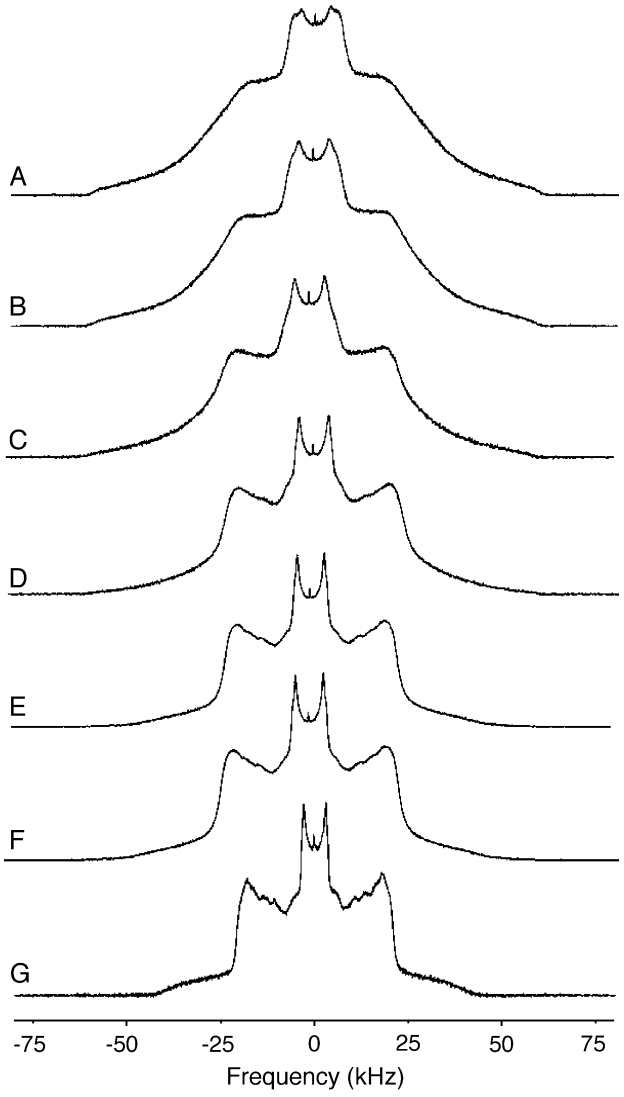


Fig. 4. Increasing concentrations of farnesol stabilize the fluid phase. $^2$H-NMR spectra of varying concentrations of farnesol-DMPC-$d_{54}$ mixtures at 16.0 °C. (A) DMPC-$d_{54}$; (B) $X_{fsl}$=0.025; (C) 0.050; (D) 0.075; (E) 0.125; (F) 0.150; (G) 0.200.

domains. At temperatures and compositions near the two-phase lines separating the two-phase region from either the fluid phase on the high-temperature side (fluidus) or from the gel phase on the low-temperature side (solidus), the domains may be quite small, making this effect even more pronounced and making it difficult to cleanly identify the phase boundaries.

The first moment provides a more quantitative description of the average orientational order in the fluid phase where $M_1$ values are proportional to the average quadrupolar splitting and to the average C–D bond order parameter, $S_{CD}$[29]. Moreover, as shown in Fig. 5, they are a sensitive measure of the onset of the phase transition or of a two-phase coexistence region. At the main phase transition of DMPC-$d_{54}$ ($T \simeq 19$ °C), there is an abrupt increase in $M_1$ by nearly a factor of two as the temperature is decreased. From an examination of Fig. 5, it is clear that this transition becomes more gradual with increasing farnesol concentration due to the emergence of the two-phase coexistence region. For temperatures and concentrations below the two-phase region, where the system is in the gel phase, the value of $M_1$ decreases markedly with increasing farnesol concentration. This reflects either an increase in the degree of molecular disorder within the gel phase, or significant changes in the rates and/or types of molecular motion which occur in the gel phase.

On the other hand, varying the concentration of farnesol in the fluid phase has little effect on the first moment. Fluid phase spectra taken at 24 °C, were numerically dePaked [31,32] to obtain the oriented spectra shown in Fig. 6a. The quadrupolar splittings of the five peaks identified in the figure were measured as a function of farnesol concentration.

Comparing the splittings observed for the sequentially numbered peaks in Fig. 6a reveals that the splitting values, $\Delta\nu_Q$, are independent of farnesol content typically to within

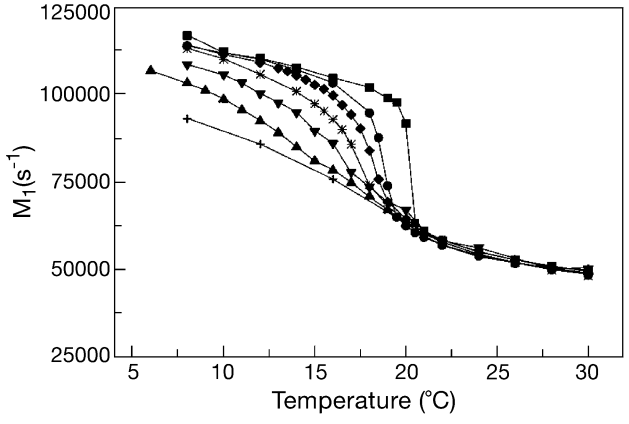


Fig. 5. Temperature dependence of the first moment ($M_1$) of the $^2$H-NMR spectra for various concentrations of farnesol-DMPC-$d_{54}$ mixtures. DMPC-$d_{54}$ (squares); $X_{fsl} = 0.025$ (circles); 0.050 (diamonds); 0.749 (stars); 0.125 (downward triangles); 0.150 (upward triangles); 0.200 (crosses). Uncertainty of the $M_1$ values is less than 1% (within the size of the symbols).

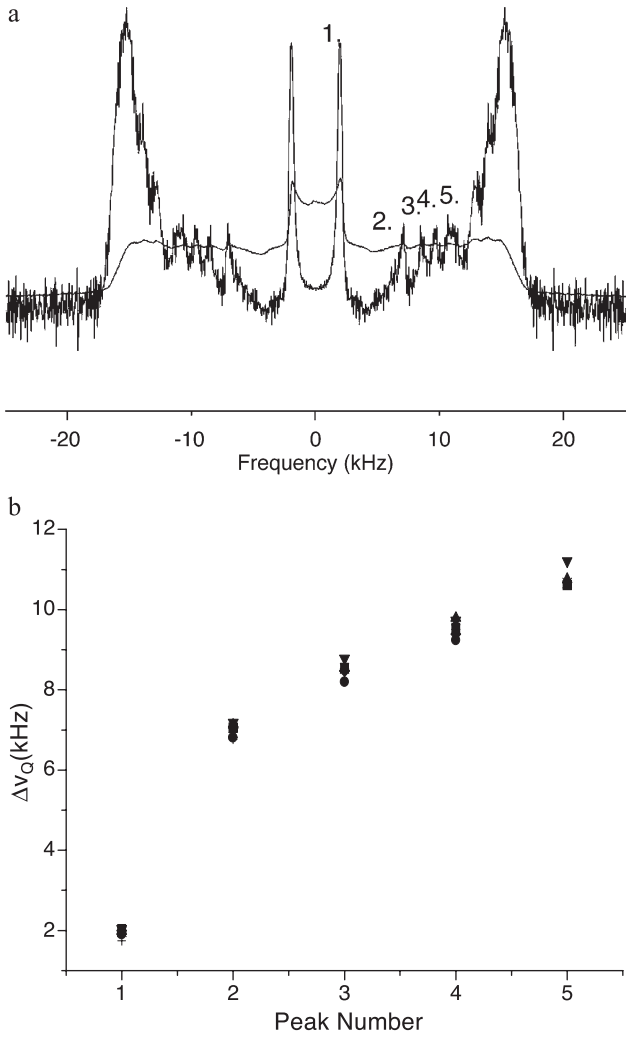


Fig. 6. (a) Depaked spectrum of DMPC-$d_{54}$ at $T = 24.0$ °C. Peaks 1–5 were identified in spectra representative of increasing concentrations of farnesol at the same temperature. (b) Quadrupolar splitting profile ($T = 24.0$ °C). DMPC$_{54}$ (squares); $X_{fsl} = 0.025$ (circles); 0.050 (diamonds); 0.749 (stars); 0.125 (downward triangles); 0.150 (upward triangles); 0.200 (crosses). Plotting the quadrupolar splitting of peaks 1–5 (as illustrated in Fig. 6a), reveals that there is negligible variation in the splittings (and therefore acyl chain order) as a function of farnesol concentration in the fluid phase.

~ 3% (except for the methyl group where the variation is approximately ± 5%), as shown in Fig. 6b. Since the fluid phase is characterized by axially symmetric reorientation of the lipids about the local bilayer normal, the mean quadrupolar splitting is proportional to the lipid hydrocarbon chain order parameter, $S_{CD}$, at the labelled position [29,30]. Thus, farnesol has a negligible effect on the orientational order of DMPC-$d_{54}$ acyl chains in the fluid phase.

These findings are in contrast to those obtained from a steady-state 1,6-diphenyl-1,3,5 hexatriene (DPH) fluorescence polarization investigation on lipids extracted from CEM-C1 cells (derived from acute T-cell leukemia cells). Using DPH as a probe, this study revealed that farnesol

induces a decrease in the fluorescence an isotropy [20]. $^{13}C$ NMR spin-lattice relaxation measurements of the effects of the similarly branched molecules, phytanic acid and vitamin E (D,L-α-tocopherol), on lecithin bilayers indicated that these compounds increase the lipid chain $^{13}C$ relaxation times above $T_m$, presumably by disrupting hydrocarbon chain packing [37]. However, a $^2H$-NMR study of the influence of the somewhat longer, saturated molecules phytol and phytanic acid on 1-palmitoyl (stearoyl)-2-[$^2H_{31}$] palmitoyl-*sn*-glycero-3-phosphocholine suggested that at concentrations of 20 mol% these compounds induce acyl chain order in the fluid phase, as they increase the mean order parameter, $<S_{CD}>$ by ~9% at 50 °C [21]. Studies of the effects of saturated alcohols of roughly equivalent length (having between 12 and 16 backbone carbons) reveal a tendency for shorter chain alcohols to slightly decrease and longer chain alcohols to slightly increase order parameters as determined by EPR spectroscopy in both egg PC/cholesterol [38] and extracted biological membranes [39]. On the other hand, alcohols with a chain length of 12 carbons were observed to exert no significant effect on order parameters in egg PC/cholesterol bilayers [38].

To gain a deeper understanding of how farnesol influences lipid phase behaviour, a temperature–composition plot was constructed and is shown in Fig. 7. By visually inspecting the spectra, the temperatures of the onset of the gel phase and disappearance of the fluid phase components were determined. The presence of a gel phase component (see expanded section in Fig. 3) is indicated by a gradual increase in intensity of the spectrum at frequencies in the frequency range from about ±32 to ±26 kHz where there is normally no intensity for a fluid phase spectrum. On the other hand, the fluid phase is easily identified by the sharp terminal methyl group 90° edges near ±3 kHz, and by the strong methylene group "plateau's" 90° edge near ±24 kHz. Thus, the fluid phase component is considered to have disappeared when the shoulders of the predominantly gel phase spectrum slope smoothly downwards to yield the characteristic bell shape. For example, for 12.5 mol% farnesol (see Fig. 3), the fluidus boundary (onset of gel phase) was determined to be at $T = 17.5 \pm 0.5$ °C while the disappearance of the fluid spectral components (solidus boundary) was determined to be at $T = 9.5 \pm 1.5$ °C. The rather subjective nature of the procedure used to identify the onset and completion temperatures of the two-phase region leads to considerable uncertainty in the determination of the phase boundaries. Starting from the fluid phase spectrum, it is quite easy to detect a very small amount of gel phase component, depending to some extent on the signal to noise ratio of the spectrum. Determining the lower limit of the two-phase region, or solidus, is considerably more difficult. Within the limitations of this procedure, the temperature–composition plot was found to exhibit a broadening of the pure lipid fluid to gel phase transition into a fluid–gel two-phase coexistence region with increasing farnesol concentration. At the higher farnesol concentrations used in this study it is possible that the system is approaching a critical concentration of farnesol beyond which the transition between gel and fluid phases becomes continuous. At 15 mol% farnesol, the $^2H$-NMR spectra still exhibit a region with a clear two-phase character, however, at the highest concentration used, 20 mol% farnesol, the spectra change more gradually and a clear coexistence is becoming difficult to establish. This analysis of phase behaviour around the main phase transition is consistent with calorimetry results ([20], Rowat and Ipsen, private communication).

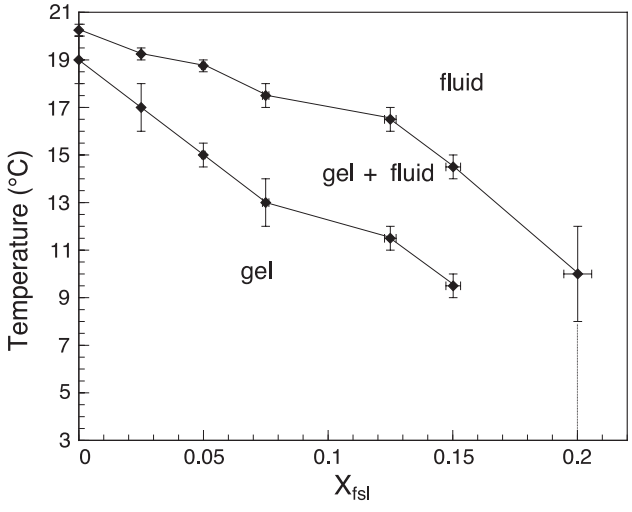


Fig. 7. Temperature–composition plot for farnesol-DMPC-$d_{54}$ [diamonds: $^2H$-NMR]. The fluid phase boundary (fluidus) was defined as the temperature at which the first onset of gel phase is observed. Disappearance of the fluid phase was used to define the gel phase boundary (solidus).

A study of the slightly longer, branched compounds phytol and phytanic acid (20 mol%) in 1-palmitoyl 1(stearoyl)-2-[$^2H_{31}$] palmitoyl-*sn*-glycero-3-phosphocholine (PC-$d_{31}$) revealed a similar decrease in onset temperature and broadening of the main phase transition [21]. While plots of $M_1$ versus temperature shown in that study are similar to those obtained for farnesol in DMPC-$d_{54}$, there is a notable exception in that incorporation of the saturated chain phytol and phytanic acid tends to increase the value of $M_1$ in the fluid phase.

It is evident that farnesol has a unique effect upon the lipid bilayer. While lowering and broadening the phase transition, farnesol leaves the quadrupolar splittings in the fluid phase unchanged (Fig. 6b), suggesting that lipid conformation, dynamics and orientational order above $T_m$ remain relatively unperturbed. This effect is in stark contrast to that due to incorporation of cholesterol and saturated fatty acids, which tend to promote more ordered lipid phases and which, like farnesol, can also be post-translationally attached to proteins. It should be noted in this regard that the fact that increasing farnesol concentration lowers the temperature of the fluidus phase boundary is a result of the preferential partitioning of farnesol into the fluid phase. Thus the lack of any influence of farnesol concentration on

lipid chain order in the fluid phase is not due to the exclusion of farnesol from that phase.

### 3.1. Farnesol versus cholesterol

The cholesterol/DPPC phase diagram exhibits a narrow two-phase region at low cholesterol concentrations, and a three-phase line between ~7 and 20 mol% cholesterol, which lies about 1° below the pure lipid chain melting transition, $T_m$ [34]. Such a phase diagram is the result of the fact that at low concentrations, cholesterol is nearly equally as soluble in the liquid disordered phase ($\ell_d$ or fluid) as it is in the solid ordered phase ($s_o$ or gel) [34,40]. At high cholesterol concentrations (i.e., ≥20 mol%), the distinct phase has a level of molecular order which is comparable to that of the $s_o$ phase but the molecules experience rapid axially symmetric reorientation about the bilayer normal and rapid lateral diffusion rates more typical of the $\ell_d$ phase. At intermediate concentrations (10–20 mol%), there is a two-phase $\ell_d$-$\ell_o$ coexistence region for temperatures just above the three-phase line, and $s_o$-$\ell_o$ phase coexistence just below the three-phase line. It is clear that at high concentrations (≥20 mol%), cholesterol favours the $\ell_o$ over the $s_o$ phase [40]. This behaviour is in contrast to that resulting from the addition of farnesol which preferentially partitions into and stabilizes the fluid ($\ell_d$) phase.

$^2$H-NMR experiments reveal a dramatic increase in the molecular order parameters (quadrupolar splittings) within the $\ell_d$ phase with increasing cholesterol concentration. Farnesol, on the other hand, is seen to have little effect upon quadrupolar splittings in the $\ell_d$ phase and induces a broad two-phase coexistence region at temperatures below the pure lipid $T_m$. It is evident that the different molecular properties of cholesterol and farnesol influence lipid behaviour in strikingly different ways.

### 3.2. Farnesol versus saturated fatty acids

Studies of saturated fatty acids—roughly equivalent in length to farnesol but lacking the branched methyl groups—reveal that 14-carbon myristic acid modifies DMPC lipid phase behaviour in a way opposite to farnesol. At similar concentrations, up to about 20 mol%, this compound promotes lipid ordering and stabilizes the gel phase, so that the onset of the fluid to gel chain melting transition increases with myristic acid concentration [41].

### 3.3. Implications

This contrast between the effects of farnesol and saturated fatty acids or cholesterol on phospholipid phase behaviour is particularly significant in the context of studies of detergent-resistant membranes (DRMs) or lipid 'rafts'. Having a composition rich in sphingolipids and cholesterol, these domains, which have been postulated to be in the liquid ordered or $\ell_o$ phase, were first detected using detergent insolubility tests [42]. Physical evidence of lateral membrane organization in both model [43–46] and biological systems [47–49] substantiate these findings (for a recent review, see Ref. [50]). Such raft domains are thought to play a role in the spatial organization of proteins important for signal transduction and membrane transport processes [51–54]. The post-translational lipid modification of proteins can act to modulate protein membrane associations. Specifically, the lipid chain which attaches to the protein potentially can determine the selective targeting of proteins to lipid domains: proteins and peptides attached to saturated chains preferentially partition into ordered lipid domains whereas prenylated proteins/peptides are excluded from these lipid domains[47,55,56]. The clustering at the nanometer scale of prenylated proteins in live cells has been detected [47], and this clustering was observed to persist even after cholesterol extraction suggesting that prenyl moieties may promote phase segregation.

In light of some of the effects on membrane phase equilibria discussed above, these observations are not surprising. It is clear that farnesol prefers the fluid ($\ell_d$) phase. In contrast, saturated fatty acids promote and stabilize the gel ($s_o$) phase. These different effects on membrane phase behaviour may provide insight into the mechanism of protein targeting to subcellular sites [47].

### 3.4. How is farnesol organized in the membrane?

This study provides insight into how lipid phase behaviour responds to the presence of farnesol. Another aspect which needs to be considered is the organization of farnesol within the lipid bilayer. Experimental evidence indicates that farnesol strongly partitions into the bilayer ([18,20]; Rowat and Ipsen, private communication). It is likely that farnesol's polar headgroup serves as an interfacial anchor, facilitating the alignment of the isoprenoid chain roughly parallel to or along the lipid acyl chains. This conformation would be in accordance with that of long chain saturated alcohols in membranes. Whether farnesol is intercalated between phospholipid chains in this fashion, or integrates instead into the bilayer interior between the two leaflets could be detected either as a decrease in phospholipid headgroup lateral density or a thickening of the bilayer using X-ray diffraction techniques.

On a mesoscopic scale, it is certain that domains of differing composition form to accommodate fluid–gel phase coexistence. Whether farnesol induces microdomain formation in the one-phase regions ($\ell_d$ or $s_o$), cannot be easily determined by NMR if molecular exchange between the domains occurs on a time scale shorter than that of the NMR experiments. In the case of fluid–fluid phase coexistence, the characteristics of the NMR spectra may be so similar that it becomes impossible to distinguish between coexisting components. The relevant NMR time scale for the detections of the effects of diffusion or exchange of lipids between coexisting domains depends on the spectro-

scopic differences characteristic of those domains. For example, if the $^2$H-NMR quadrupolar splitting in one domain is 10 kHz larger than in another, then an approximate time scale of 0.1 ms is defined by this difference. If the difference in quadrupolar splittings is only 1 kHz, then the effective time scale is 10 times longer (1 ms). The shorter the time scale the less important such diffusion effects become, and the smaller the domain size necessary before those effects become visible in the NMR spectrum.

While we cannot yet establish whether or not such microdomains are formed, we can estimate a lower limit on the size of any microdomain by considering the root mean squared distance a lipid can diffuse during the NMR time scale. In the case of the fluid phase, where we see sharply defined quadrupolar powder pattern line shapes, we can define this time scale to be approximately equal to the transverse relaxation time, $T_2$, which typically has values of less then 0.5–1 ms [30]. During this length of time, using the typical fluid phase lateral diffusion constant $D \approx 5 \times 10^{12}$ m$^2$/s, a lipid molecule can diffuse about 100 nm. If the domains are smaller than this, we would expect to see a single average environment. If the domains were significantly larger than this we would potentially see two environments, provided that the lipids in the two environments had measurably different degrees of chain order. Experimentally, except for within the fluid–gel two-phase coexistence region, we see one average environment. This could indicate either the existence of one average environment or two environments which have very similar degrees of chain order (for example, a fluid–fluid coexistence region). It should be noted that the clustering of prenylated proteins in live cells has been detected at the nanometer scale [47]. The existence of isoprenoid domains would indeed substantiate these observations and theories of lipid-driven protein targeting.

It is notable that the quadrupolar splittings, which are proportional to the degree of acyl chain order [30] and correlated to the bilayer thickness[57,58], remain unchanged in the fluid phase ($T$=24 °C). In a biological context, the existence of microdomains within the fluid phase would suggest that farnesol could modulate the membrane association of proteins without dramatically perturbing membrane structure.

## 4. Conclusion

This $^2$H-NMR investigation of farnesol in DMPC-$d_{54}$ membranes demonstrates how this 15-carbon isoprenoid affects lipid phase behaviour. Increasing concentrations of farnesol (up to 20 mol%) progressively decrease and broaden the main phase transition region indicating the emergence of a fluid–gel phase coexistence region. This is quantified by the temperature–composition plot presented here. In the coexistence region, below the chain-melting transition temperature of the pure lipid, $^2$H-NMR spectra consist of a superposition of two components, one characteristic of the $W_d$ or fluid phase, the other of the $s_o$ or gel phase. As a result, the values of $M_1$ within the coexistence region are smaller than those seen at the same temperature in the $s_o$ phase. The variation of the fluid phase component of the spectrum in this two-phase region with sample composition suggests that molecular exchange between fluid and gel phase domains is important, especially near the phase boundaries where domain size might be expected to be small. Well within the gel phase the value of $M_1$ is quite sensitive to the farnesol concentration, suggesting a significant influence on molecular motion and/or molecular order within that phase. In the fluid phase, however, the quadrupolar splittings ($\Delta\nu_Q$) and $M_1$ values are independent of farnesol concentration. Investigations by $^{13}$C-NMR or $^2$H-NMR of deuterated farnesol would help to elucidate farnesol's conformation and dynamics throughout all regions of the temperature–composition plot. Further studies of this model system will continue to provide valuable insight into the fundamentals of lipid–isoprenoid interactions occurring in membranes.

## Acknowledgements

We would like to thank Ms. Valerie Robertson and Ms. Lesley Foley of the University of Guelph's Food and Soft Materials NMR Centre for their technical assistance. We also would like to thank Dr. J.H. Ipsen for helpful discussions. ACR is a Julie Payette Scholar sponsored by the Natural Sciences and Engineering Research Council (NSERC) of Canada. This study was also funded by grants from NSERC and the Canadian Foundation for Innovation (CFI). MEMPHYS-Centre for Biomembrane Physics is supported by the Danish National Research Foundation.

## References

[1] J.B. Roullet, H. Xue, J. Chapman, P. McDougal, C.M. Roullet, D.A. McCarron, Farnesyl analogues inhibit vasoconstriction in animal and human arteries, J. Clin. Invest. 97 (1996) 2384–2390.
[2] J.B. Roullet, U.C. Luft, H. Xue, J. Chapman, R. Bychkov, C.M. Roullet, F.C. Luft, H. Haller, D.A. McCarron, Farnesol inhibits L-type $Ca^{2+}$ channels in vascular smooth muscle cells, J. Biol. Chem. 272 (1997) 32240–32446.
[3] E. Pongo, Z. Balla, K. Mubagwa, W. Flameng, I. Edes, Z. Szilvassy, P. Ferdinandy, Deterioration of the protein kinase C-$K_{ATP}$ channel pathway in regulation of coronary flow in hypercholesterolaemic rabbits, Eur. J. Pharmacol. 418 (2001) 217–223.
[4] A. Bringmann, S.N. Skatchkov, F. Faude, V. Enzmann, A. Reichenbach, Farnesol modulates membrane currents in human retinal glial cells, J. Neurosci. Res. 62 (2000) 396–402.
[5] I. Adany, E.M. Yazlovitskaya, J.S. Haug, P.A. Voziyan, G. Melnykovych, P.A. Voziyan, Differences in sensitivity to farnesol toxicity between neoplastically- and non-neoplastically-derived cells in culture, Cancer Lett. 79 (1994) 175–179.
[6] A. Rioja, A.R. Pizzey, C.M. Marson, N.S.B. Thomas, Preferential induction of apoptosis of leukaemic cells by farnesol, FEBS Lett. 467 (2000) 291–295.
[7] J.S. Haug, C.M. Goldner, E.M. Yazlovitskaya, P.A. Voziyan, G.

Melnykovych, Directed cell-killing (apoptosis) in human lymphoblastoid cells incubated in the presence of farnesol—effect of phosphatidylcholine, Biochim. Biophys. Acta 1223 (1994) 133–140.
[8] T.E. Meigs, D.S. Roseman, R.D. Simoni, Regulation of 3-hydroxy-3-methylglutaryl-coenzyme. A reductase degradation by the nonsterol mevalonate metabolite farnesol in vivo, J. Biol. Chem. 271 (1996) 7916–7922.
[9] C.C. Correll, L. Ng, P.A. Edwards, Identification of farnesol as the non-sterol derivative of mevalonic acid required for the accelerated degradation of 3-hydoxy-3-methylglutaryl-coenzyme A reductase, J. Biol. Chem. 269 (1994) 17390–17393.
[10] D.L. Bradfute, R.D. Simoni, Non-sterol compounds that regulate cholesterogenesis, J. Biol. Chem. 269 (1994) 6645–6650.
[11] K. Hanley, L.G. Kömüves, D.K. Ng, K. Schoonjans, S.S. He, P. Lau, D.D. Bikle, M.L. Williams, P.M. Elias, J. Auwerx, K.R. Feingold, Farnesol stimulates differentiation in epidermal keratinocytes via PPARα, J. Biol. Chem. 275 (2000) 11484–11491.
[12] N. Takahashi, T. Kawada, T. Goto, T. Yamamoto, A. Taimatsu, N. Matsui, K. Kimura, M. Saito, M. Hosokawa, K. Miyashita, T. Fushiki, Dual action of isoprenols from herbal medicine son both PPARγ and PPARα in 3T3-L1 adipocytes and HepG2 hepatocytes, FEBS Lett. 514 (2002) 315–322.
[13] M. Sinensky, Functional aspects of polyisoprenoid protein substituents: roles in protein–protein interaction and trafficking, Biochim. Biophys. Acta 1529 (2000) 203–209.
[14] M. Sinensky, Recent advances in the study of prenylated proteins, Biochim. Biophys. Acta 1484 (2000) 93–106.
[15] P.J. Casey, Protein lipidation in cell signaling, Science 268 (1995) 221–225.
[16] M.A. McCloskey, F.A. Troy, Paramagnetic isoprenoid carrier lipids: 1. Chemical synthesis and incorporation into model membranes, Biochemistry 19 (1980) 2056–2060.
[17] M.A. McCloskey, F.A. Troy, Paramagnetic isoprenoid carrier lipids: 2. Dispersion and dynamics in lipid membranes, Biochemistry 19 (1980) 2061–2066.
[18] J.S. de Ropp, F.A. Troy, Chemical synthesis and $^{2}$H-NMR investigations of polyisoprenols: dynamics in model membranes, Biochemistry 23 (1984) 2691–2695.
[19] J.S. de Ropp, F.A. Troy, $^{2}$H-NMR investigation of the organization and dynamics of polyisoprenols in membranes, J. Biol. Chem. 260 (1985) 15669–15674.
[20] O.P. Bondar, G. Melnykovyck, E.S. Rowe, Effects of farnesol on the thermotropic behaviour of dimyristoylphosphatidylcholine, Chem. Phys. Lipids 74 (1994) 93–98.
[21] J. Yue, J.L. Thewalt, R.J. Cushley, Deuterium nuclear magnetic resonance study of the interaction of branched chain compounds (phytanic acid, phytol) with a phospholipid model membrane, Chem. Phys. Lipids 49 (1988) 205–213.
[22] T. Byström, E. Strandberg, F.A. Kovacs, T.A. Cross, G. Lindblom, Influence of trans membrane peptides on bilayers of phosphatidylcholines with different acyl chain lengths studied by solid-state NMR, Biochim. Biophys. Acta 1509 (2000) 335–345.
[23] G.G. McManus, G.W. Buchanan, H.C. Jarrell, R.M. Epand, R.F. Epand, J.J. Cheetham, Membrane perturbing properties of sucrose polyesters, Chem. Phys. Lipids 109 (2001) 185–202.
[24] M.R. Morrow, D. Singh, D. Lu, C.W.M. Grant, Glycosphingolipid fatty acid arrangement in phospholipid bilayers: cholesterol effects, Biophys. J. 68 (1995) 179–186.
[25] N. Kitson, M. Monck, K. Wong, J. Thewalt, P. Cullis, The influence of cholesterol 3-sulphate on phase behaviour and hydrocarbon order in model membrane systems, Biochim. Biophys. Acta 1111 (1992) 127–133.
[26] D. Lu, D. Singh, M.R. Morrow, C.W. Grant, Effect of glycosphingolipid fatty acid chain length on behaviour of unsaturated phosphatidylcholine bilayers: a $^{2}$H-NMR study, Biochemistry 32 (1993) 290–297.
[27] J.H. Davis, K.R. Jeffrey, M. Bloom, M.I. Valic, T.P. Higgs, Quadrupolar echo deuteron magnetic resonance spectroscopy in ordered hydrocarbon chains, Chem. Phys. Lett. 42 (1976) 3390–3394.
[28] R.S. Prosser, J.H. Davis, F.W. Dahlquist, M.A. Lindorfer, $^{2}$H nuclear magnetic resonance of the gramicidin. A backbone in a phospholipid bilayer, Biochemistry 30 (1991) 4687–4696.
[29] J.H. Davis, K.R. Jeffrey, M. Bloom, Spin-lattice relaxation as a function of chain position in perdeuterated potassium palmitate, J. Magn. Reson. 29 (1978) 191–199.
[30] J.H. Davis, The description of membrane lipid conformation, order, and dynamics by $^{2}$H-NMR, Biochim. Biophys. Acta 737 (1983) 117–171.
[31] M. Bloom, J.H. Davis, A.L. Mackay, Direct determination of the oriented sample NMR spectrum from the powder spectrum for systems with local axial symmetry, Chem. Phys. Lett. 80 (1981) 198–202.
[32] E. Sternin, M. Bloom, A.L. MacKay, De-pake-ing of NMR spectra, J. Magn. Res. 55 (1983) 274–282.
[33] M.R. Morrow, R. Srinivasan, N. Grandal, The phase diagram of dimyristoylphosphatidylcholine and chain-perdeuterated distearoylphosphatidylcholine: a deuterium NMR spectral difference study, Chem. Phys. Lipids 58 (1991) 63–72.
[34] M.R. Vist, J.H. Davis, Phase-equilibria of cholesterol dipalmitoylphospatidylcholine mixtures—$^{2}$H nuclear magnetic resonance and differential scanning calorimetry, Biochemistry 29 (1990) 451–464.
[35] J.C. Huschilt, R.S. Hodges, J.H. Davis, Phase equilibria in an amphiphilic peptide-phospholipid model membrane by deuterium nuclear magnetic resonance difference spectroscopy, Biochemistry 24 (1985) 1377–1386.
[36] M.R. Morrow, J.C. Huschilt, J.H. Davis, Simultaneous modeling of phase and calorimetric behaviour in an amphiphilic peptide/phospholipid model membrane, Biochemistry 24 (1985) 5396–5406.
[37] R.J. Cushley, B.J. Forrest, Structure and stability of vitamin E-lecithin and phytanic acid-lecithin bilayers studied by $^{13}$C and $^{31}$P nuclear magnetic resonance, Can. J. Chem. 55 (1977) 220–226.
[38] D.E. Raines, S.E. Korten, W.A.G. Hill, K.W. Miller, Anesthetic cutoff in cycloalkanemethanols: a test of current theories, Anesthesiology 78 (1993) 918–927.
[39] K.W. Miller, L.L. Firestone, J.K. Alifimoff, P. Streicher, Nonaesthetic alcohols dissolve in synaptic membranes without perturbing their lipids, Proc. Natl. Acad. Sci. U. S. A. 86 (1989) 1084–1087.
[40] J.H. Ipsen, G. Karlström, O.G. Mouritsen, H. Wennerström, M.J. Zuckermnn, Phase equilibria in the phosphatidylcholine–cholesterol system, Biochim. Biophys. Acta 905 (1987) 162–172.
[41] R. Koynova, B. Tenchov, G. Rapp, Mixing behaviour of saturated short-chain phosphatidylcholines and fatty acids: eutectic points, liquid and solid phase immiscibility, non-lamellar phases, Chem. Phys. Lipids 88 (1997) 45–61.
[42] E. London, D.A. Brown, Insolubility of lipids in triton X-100: physical origin and relationship to sphingolipid/cholesterol membrane domains (rafts), Biochim. Biophys. Acta 1508 (2000) 182–195.
[43] L.A. Bagatolli, Direct observation of lipid domains in free standing bilayers: from simple to complex lipid mixtures, Chem. Phys. Lipids 122 (2003) 137–145.
[44] J.R. Silvius, Fluorescence energy transfer reveals microdomain formation at physiological temperatures in lipid mixtures modeling the outer leaflet of the plasma membrane, Biophys. J. 85 (2003) 1034–1045.
[45] A.V. Samsanov, I. Mihalyov, F.S. Cohen, Characterization of cholesterol-sphingomyelin domains and their dynamics in bilayer membranes, Biophys. J. 81 (2001) 1486–1500.
[46] H.A. Rinia, B. de Kruijff, Imaging domains in model membranes with atomic force microscopy, FEBS Lett. 504 (2001) 194–199.
[47] D.A. Zacharias, J.D. Violin, A.C. Newton, R.Y. Tsien, Partitioning of lipid-modified monomeric GFPs into membrane microdomains of live cells, Science 296 (2002) 913–916.
[48] F.R. Maxfield, Plasma membrane microdomains, Curr. Opin. Cell Biol. 14 (2002) 483–487.
[49] C. Dietrich, L.A. Bagatolli, Z.N. Volovyk, N.L. Thompson, M. Levi, K.

Jacobson, E. Gratton, Lipid rafts reconstituted in model membranes, Biophys. J. 80 (2001) 1417–1428.
[50] M. Edidin, The state of lipid rafts: from model membranes to cells, Annu. Rev. Biophys. Biomol. Struct. 32 (2003) 257–283.
[51] J.C.M. Holthuis, G. van Meer, K. Huitema, Lipid microdomains, lipid translocation and the organization of intracellular membrane transport (review), Mol. Membr. Biol. 20 (2003) 231–241.
[52] E. Ikonen, Roles of lipid rafts in membrane transport, Curr. Opin. Cell Biol. 13 (2001) 470–477.
[53] K. Simons, E. Ilkonen, Functional rafts in cell membranes, Nature 387 (1997) 569–572.
[54] D.A. Brown, E. London, Functions of lipid rafts in biological membranes, Annu. Rev. Cell Dev. Biol. 14 (1998) 111–136.
[55] S. Moffett, D.A. Brown, M.E. Linder, Lipid-dependent targeting of G proteins into rafts, J. Biol. Chem. 275 (2000) 2191–2198.
[56] K.A. Melkonian, A.G. Ostermeyer, J.Z. Chen, M.G. Roth, D.A. Brown, Role of lipid modifications in targeting proteins to detergent-resistant membrane rafts. Many raft proteins are acylated, while few are prenylated, J. Biol. Chem. 274 (1999) 3910–3917.
[57] J.H. Ipsen, O.G. Mouritsen, M. Bloom, Relationships between lipid membrane area, hydrophobic thickness, and acyl-chain orientational order: the effects of cholesterol, Biophys. J. 57 (1990) 405–412.
[58] H. Schindler, J. Seelig, Deuterium order parameters in relation to thermodynamic properties of a phospholipid bilayer. A statistical mechanical interpretation, Biochemistry 14 (1975) 2283–2287.